ISSN 1330-3651 (Print), ISSN 1848-6339 (Online)
https://doi.org/10.17559/TV-20150707172830

TIME-PERIODIC INCOMPRESSIBLE FLOW SIMULATION USING NON-LINEAR FREQUENCY DOMAIN APPROACH

M. H. Shojaeefard, A. Khorampanahi, M. Kharati Koopaee

Original scientific paper
The capability of nonlinear reduced frequency domain (NLFD) approach in predicting the flow field of time-periodic incompressible flow is investigated. The efficient NLFD method uses Fourier series representation in time considering the assumption of solution periodicity and the resulting nonlinear equations are solved using pseudo-spectral approach. In this manner, the desired periodic solution can directly be obtained without the need to solve the initial transient part. Thus, without loss of generality a considerable computational cost reduction can be achieved in comparison with the common time-accurate methods. In the present algorithm (INLFD) the NLFD approach is used to solve the flow field in an incompressible formulation and the validation is performed using some periodic test cases with analytical solutions. The results show that capturing only a limited number of temporal modes can provide an accurate estimation of the flow field. Finally, the computational costs of the INLFD and a time-accurate method are also compared which demonstrate the efficiency of the INLFD method in representing nonlinear flow field physics by savings in computational time up to 50 percent.

Keywords: *incompressible flow; non-linear reduced frequency; pressure Poisson; pseudo-spectral; time-periodic*

Simulacija vremenski periodičnog nestlačljivog toka pristupom ne-linearnog područja frekvencije

Izvorni znastveni članak
Istražuje se mogućnost predviđanja polja protoka vremenski periodičnog nestlačljivog toka pristupom područja nelinearne smanjene frekvencije - nonlinear reduced frequency domain (NLFD). Učinkovita NLFD metoda koristi predstavljanje Fourierovih serija u vremenu smatrajući da se pretpostavka periodičnosti rješenja i rezultirajuće nelinearne jednadžbe rješavaju pseudo-spektralnim pristupom. Na taj se način željeno periodičko rješenje može dobiti direktno bez potrebe rješenja inicijalnog tranzijentnog dijela. Tako se može postići značajno smanjenje troška bez gubitka generalizacije u usporedbi s uobičajenim vremenski preciznim metodama. U postojećem algoritmu (INLFD), NLFD pristup je primijenjen za rješavanje polja protoka u nestlačljivoj formulaciji a validacija se obavlja primjenom nekih periodičnih slučajeva ispitivanja s analitičkim rješenjima. Rezultati pokazuju da se obuhvatom samo ograničenog broja temporalnih načina može osigurati točna procjena polja protoka. Konačno, troškovi izračuna INFLED-a i vremenski točne metode također su uspoređeni i pokazuju učinkovitost INFLED metode u predstavljanju fizike nelinearnog polja protoka uštedom vremena izračuna do 50 posto.

Ključne riječi: *nestlačljivi tok; ne-linearno reducirana frekvencija; Poissonov tlak; pseudo-spektralan; vremenski periodičan*

1 Introduction

Despite improvements in steady flow simulations, efficient modelling of unsteady flow has been yet a challenge in computational fluid dynamics. In numerical simulation of unsteady flow, the solution time history must be resolved accurately. Thus, the added dimension (time) increases the computational cost effectively. In time-accurate solvers the equations are discretized in space and the time term is left. This would construct a coupled ordinary differential equations system. In order to resolve the solution time history, the method of advancing in time (method of lines) must be used.

By decaying the initial transient state, some unsteady flows reach a periodic steady state solution. In many of these flows, the periodic solution is of more interest than the initial transient one. Since the time which is needed to reach the periodic solution is usually much larger than the steady state period, most of the computational time is spent on resolving the initial transient solution [1].

In order to reduce the long computational time of solving the periodic unsteady flow field, periodic methods can be used. In this approach the periodic solution is calculated directly while the transient decay is not a component of the solution. Considering the solution periodicity, these methods use trigonometric interpolants such as Fourier series instead of the periodic solution which results in a spectral temporal accuracy of the solution versus the number of harmonics used [2-4]. Periodic methods can be subdivided into three main categories: linearized, semi-nonlinear and non-linear frequency domain methods.

The least expensive approach in calculation of these types of flows is to linearize the flow field about the mean flow steady solution with the assumption that the unsteady (perturbed) component magnitude is much smaller than that of the steady one. In linearized frequency domain methods the mean flow components of the solution are solved first. Any temporal frequency of the solution can then be solved from mean flow components [5]. This method has been also extended to potential, Euler and full Navier-Stokes equations for any regime of flow (subsonic, transonic and supersonic) [6-10].

However, the linearized frequency domain methods cannot adequately account for the strong nonlinearities which are typically encountered in flows. To overcome the error associated with the linearized form, semi-nonlinear and nonlinear forms of frequency domain approach have been developed. In [11-15] semi-nonlinear frequency domain analysis of periodic unsteady flow has been extended. Adamczyk [11] formed deterministic stress terms, using several different linearization and averaging operators and then modelled these terms. These terms effort to quantify the unsteady field effects on the time averaged solution. Ning et al. [12], He et al. [13] and Chen et al. [14] also used averaging operators to form the deterministic stress terms and calculated these terms with a modified version of a linearized frequency domain solver. In deterministic-stress methods, no direct coupling between the harmonics is evident mathematically. So, this method will poorly represent a physical phenomenon wherein significant energy is transferred between different harmonics.

An efficient periodic solution of fully non-linear system of equations was first proposed by Hall et al. [16] using the harmonic balance technique on 2-D turbomachinery cascades. McMullen et al. [17-19] also proposed a nonlinear frequency domain method (NLFD) which represents a form of residual in the frequency domain. He focused on 2-D turbomachinery flows and demonstrated the efficiency of this technique to represent complex non-linear flow solutions using a minimum number of harmonic modes. He [4] also showed that flow simulation in frequency domain is an order of magnitude faster than in time domain for the same level of temporal accuracy.

In spectral methods the approximations are defined in terms of a truncated series expansion, such as some quantity (error or residual) which is forced to be zero in an approximate sense [20-22]. In NLFD method, considering the assumption of periodicity in time, the state vector and fluxes can be represented by truncated Fourier series expansions. The fluxes are evaluated through spatial discretization methods and then transformed to frequency domain by a fast Fourier transform (FFT) technique. The state vector is updated in the frequency domain and transformed back to the time domain.

Murman [23] used the procedure followed by Hall et al. [15] and extended the application to 3-D Euler equations to calculate dynamic stability derivatives of some configurations in an inviscid flow. Also, the results show that in some cases for viscous flows, the solution with just a single mode would generally be irrelevant and higher (but a limited) number of modes should be considered. Mavriplis et al. [24] has also shown that only capturing the dominant modes can provide accurate estimations of fluid properties.

Kharati et al. [25, 26] have also used perturbation technique in nonlinear frequency domain method to estimate the solution at high harmonics in transonic flows. The density and velocity field at high harmonics are perturbed about those of low harmonics to form semi-linear governing equations. The proposed method has reduced the computational time in comparison with common nonlinear frequency domain approaches.

All previous researches have used non-linear reduced frequency approach in compressible form which solves energy equation alongside with momentum and continuity (or pressure) equations. However, by using incompressible form the energy equation does not need to be solved which results in numerical cost reduction. The innovation of this research is to develop a CFD code which simulates unsteady periodic incompressible flows using non-linear reduced frequency approach (INLFD code).

2 Methodology

2.1 Governing equations

The primitive variable formulation of the incompressible Navier-Stokes equations in the absence of body forces are given by Eq. (1).

$$\nabla \boldsymbol{u} = 0 \tag{1a}$$

$$\frac{\partial \boldsymbol{u}}{\partial t} + \boldsymbol{u}\cdot\nabla\boldsymbol{u} = -\frac{1}{\rho}\nabla p + \nu\nabla^2\boldsymbol{u} \tag{1b}$$

where $\boldsymbol{u}$, p, ρ and ν are velocity field, pressure, density and kinematic viscosity, respectively.

The conservative two-dimensional form of Eqs. (1a) and (1b) can be written in Cartesian coordinates as

$$u\frac{\partial u}{\partial x} + \frac{\partial v}{\partial y} = 0 \tag{2a}$$

$$\frac{\partial u}{\partial t} + \frac{\partial (uu)}{\partial x} + \frac{\partial (uv)}{\partial y} = -\frac{1}{\rho}\frac{\partial p}{\partial x} + \nu\left(\frac{\partial^2 u}{\partial x^2} + \frac{\partial^2 u}{\partial y^2}\right) \tag{2b}$$

$$\frac{\partial v}{\partial t} + \frac{\partial (uv)}{\partial x} + \frac{\partial (vv)}{\partial y} = -\frac{1}{\rho}\frac{\partial p}{\partial y} + \nu\left(\frac{\partial^2 v}{\partial x^2} + \frac{\partial^2 v}{\partial y^2}\right) \tag{2c}$$

where u and v are respectively x and y-components of the velocity vector $\boldsymbol{u}$.

Integrating Eqs. (2b) and (2c), over a control volume V and using finite volume approach in which the continuous surface integrals are represented by a discrete summation of fluxes across a finite number of control surfaces, the semi-discrete Eqs. (3.a) and (3.b) will be obtained.

$$V\frac{\partial u}{\partial t} + \sum_{C.S.}\left[\left(u^2+p\right)S_x + uvS_y\right] - \sum_{C.S.}\nu\left(\frac{\partial u}{\partial x}S_x + \frac{\partial u}{\partial y}S_y\right) = 0 \tag{3a}$$

$$V\frac{\partial v}{\partial t} + \sum_{C.S.}\left[uvS_x + \left(v^2+p\right)S_y\right] - \sum_{C.S.}\nu\left(\frac{\partial v}{\partial x}S_x + \frac{\partial v}{\partial y}S_y\right) = 0 \tag{3b}$$

where S_x and S_y are projected surfaces of control volume in x and y directions, respectively.

Let $\boldsymbol{W}=[u,v]^{\mathrm{T}}$ denote the answer vector. Also the spatial operator $\boldsymbol{R}$ is introduced as a function of space and time including both the convective and dissipative fluxes (Eq. (4)).

$$\boldsymbol{R} = \begin{bmatrix} R_x \\ R_y \end{bmatrix} = \begin{bmatrix} \sum_{C.S.}\left[\left(u^2+p\right)S_x + uvS_y\right] - \sum_{C.S.}\nu\left(\frac{\partial u}{\partial x}S_x + \frac{\partial u}{\partial y}S_y\right) \\ \sum_{C.S.}\left[\left(v^2+p\right)S_y + uvS_x\right] - \sum_{C.S.}\nu\left(\frac{\partial v}{\partial x}S_x + \frac{\partial v}{\partial y}S_y\right) \end{bmatrix} \tag{4}$$

So the momentum equations are simplified in a semi-discrete form:

$$V\frac{\partial \boldsymbol{W}}{\partial t} + \boldsymbol{R} = 0 \tag{5}$$

2.2 Transformation of equations into frequency domain

Considering the assumption of periodicity of the solution vector $\boldsymbol{W}$ and spatial operator $\boldsymbol{R}$ in time, both can be represented by truncated Fourier series expansions:

$$\boldsymbol{W} = \sum_{k=-\frac{N-1}{2}}^{\frac{N-1}{2}} \hat{\boldsymbol{W}}_k e^{ik\omega t} \tag{6a}$$

$$\boldsymbol{R} = \sum_{k=-\frac{N-1}{2}}^{\frac{N-1}{2}} \hat{\boldsymbol{R}}_k e^{ik\omega t} \tag{6b}$$

where $i^2=-1$.

Since the trial (or basis) functions $exp(ik\omega t)$ are known, determination of the expansion coefficients, $\hat{\boldsymbol{W}}_k$ and $\hat{\boldsymbol{R}}_k$, yields acquiring $\boldsymbol{W}$ and $\boldsymbol{R}$. Therefore, each of the Eqs. (6a) and (6b) would contain N complex coefficients which have to be determined. Since the functions $\boldsymbol{W}$ and $\boldsymbol{R}$ are assumed to be real, two Fourier coefficients with an opposite value of k, are complex conjugate, i.e., $\hat{\boldsymbol{W}}_{-k}=\hat{\boldsymbol{W}}_k$ and $\hat{\boldsymbol{R}}_{-k}=\hat{\boldsymbol{R}}_k$.

The coefficients $\hat{\boldsymbol{W}}_0$ and $\hat{\boldsymbol{R}}_0$ being obviously real, the expansions (6) would contain N real unknowns. Eq. (7) is also obtained by substituting these discrete Fourier series into Eq. (5).

$$V\frac{\partial}{\partial t}\left[\sum_{k=-\frac{N-1}{2}}^{\frac{N-1}{2}} \hat{\boldsymbol{W}}_k e^{ik\omega t}\right] + \sum_{k=-\frac{N-1}{2}}^{\frac{N-1}{2}} \hat{\boldsymbol{R}}_k e^{ik\omega t} = 0 \tag{7}$$

Moving time derivative inside the series summation and using Fourier terms orthogonality property, Eq. (8) is obtained for each wave number k. In the absence of time derivative term, this equation can be solved just like a steady equation.

$$ikV\omega\hat{\boldsymbol{W}}_k + \hat{\boldsymbol{R}}_k = 0 \tag{8}$$

Since $\boldsymbol{R}$ is a nonlinear function of $\boldsymbol{W}(t)$, due to convective terms, each coefficient $\hat{\boldsymbol{R}}_k$ depends on all answer transform coefficients, $\hat{\boldsymbol{W}}_k$. Thus, Eq. (8) represents a nonlinear set of equations which must be solved iteratively.

Here is a problem of expressing each $\hat{\boldsymbol{R}}_k$ in terms of all coefficients, $\hat{\boldsymbol{W}}_k$ Hall proposed two approaches to calculate these coefficients [16]. In the first approach $\hat{\boldsymbol{R}}_k$ is directly calculated from all $\hat{\boldsymbol{W}}_k$ using a complex series of convolution sums, which has a massive complexity and computational cost. The second procedure is to use a pseudo-spectral method which relies on the computational efficiency of FFT. This approach is described in the following section.

The other problem to calculate $\boldsymbol{R}$ in incompressible formulation arises from the unknown pressure field, p. There is no explicit equation to obtain pressure, however, the pressure field can be calculated indirectly. Substituting the correct pressure field into momentum equations, the resulting velocity field would satisfy the continuity equation. So, an additional equation which is referred to as pressure Poisson equation (PPE) must be solved. This equation is derived from taking the momentum Eq. (1b) divergence along with continuity Eq. (1a):

$$\Delta p = -\rho\nabla\cdot\left(\boldsymbol{u}\cdot\nabla\boldsymbol{u}\right) \tag{9}$$

So the correct velocity and pressure field can be obtained by solving momentum and pressure Poisson equations iteratively.

The resultant PPE formulation in conjugate with the momentum equation is equivalent to a set of continuity and momentum equations if and only if proper boundary conditions for pressure are specified such that the velocity divergence becomes zero ($\nabla\boldsymbol{u}=0$) at the boundaries (theorem 1 in [27]). Projecting the momentum equation on the normal vector $\boldsymbol{n}$ at the boundaries, the Neumann boundary condition would be obtained [27-28]:

$$\frac{\partial p}{\partial \boldsymbol{n}} = \boldsymbol{n}\cdot\left[-\frac{\partial \boldsymbol{u}}{\partial t} - \boldsymbol{u}\cdot\nabla\boldsymbol{u} + \nu\nabla^2\boldsymbol{u}\right], \text{ on boundaries.} \tag{10}$$

2.3 Solution procedure

The goal is to achieve a solution, $\boldsymbol{W}$, for which the system of Eqs. (8) converges to zero for all wave numbers. However, at any iteration during the solution process, the unsteady residual, $\hat{\boldsymbol{I}}_k$ which is defined in Eq. (11), has a finite value.

$$\hat{\boldsymbol{I}}_k = ikV\omega\hat{\boldsymbol{W}}_k + \hat{\boldsymbol{R}}_k \tag{11}$$

In order to calculate $\hat{\boldsymbol{R}}_k$ in terms of $\hat{\boldsymbol{W}}_k$ (for all k), the pseudo-spectral method is used. The first assumption in this method is that $\hat{\boldsymbol{W}}_k$ is known for all wave numbers. Using inverse FFT, the coefficients $\hat{\boldsymbol{W}}_k$ transform back to physical space resulting in a state vector, $\boldsymbol{W}(t)$ which is sampled at evenly distributed intervals over the time period. The spatial operator $\boldsymbol{R}$ at each time instance can then be computed from the known $\boldsymbol{W}(t)$ and the pressure p(t), which is obtained by solving the PPE. FFT is also used to transform the spatial operator into the frequency domain. So $\hat{\boldsymbol{R}}_k$ would be obtained for all wave numbers. In order to compute the unsteady residual $\hat{\boldsymbol{I}}_k$ at each wave number, $\hat{\boldsymbol{R}}_k$ is added to the spectral representation of the temporal derivative $ikV\omega\hat{\boldsymbol{W}}_k$. A diagram of the transformations used by the pseudo spectral approach for one iteration is shown in Fig. 1.

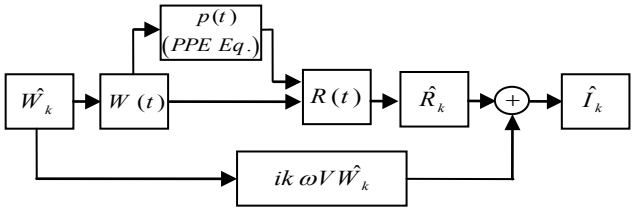

Figure 1 The pseudo-spectral approach diagram for incompressible flows

The spatial operators computational cost in pseudo-spectral approach is the product of one steady-state spatial operator cost and the number of time instances used to represent the solution, N. Also, the cost of FFT is proportional to $Nln(N)$ [16]. So, for more practical values

of N (under 10) the pseudo-spectral approach cost is mainly determined by the cost associated with the calculation of spatial operators.

One of the advantages of the pseudo-spectral approach is its flexibility in adopting different forms of non-linear operators. In this research the finite volume formulation is used, however the application of the pseudo-spectral approach is also well suited for finite difference or other types of spatial operators. In addition, different turbulence models which would be difficult to be explicitly expressed in the frequency domain are more easily handled in the pseudo-spectral approach.

2.4 Pseudo-time derivatives

Instead of solving Eq. (11) directly a pseudo-time derivative can be added to the unsteady residual. The application of the pseudo-time derivative is consistent with established convergence acceleration techniques used to solve steady-state problems [16]. Adding this term, a time-stepping approach can be employed to numerically integrate the resulting Eq. (12).

$$V\frac{\partial \hat{\boldsymbol{W}}_k}{\partial \tau}+\hat{\boldsymbol{I}}_k=0 \tag{12}$$

In Eq. (12) the pseudo-time derivative acts as a gradient to drive the absolute value of the unsteady residual to zero for each wave number.

2.5 Staggered grid

In order to overcome the problem of oscillating pressure field, a staggered grid arrangement is used in which the scalar variables (pressure data) are located at the cell centres of the control volume, whereas the velocity and momentum variables (u and v velocities) are placed on the cell faces. This is different from a collocated grid arrangement, where all variables are stored in the same position and a finite volume-based discretization employs special interpolation schemes to determine the flux across the cell edges. A staggered storage is mainly used on structured grids. Using a staggered grid is a simple way to avoid odd-even decoupling between the pressure and velocity. Odd-even decoupling is a discretization error which can occur on collocated grids and can then lead to a decoupled (checkerboard) pressure field and oscillations in solutions [29-30].

3 Test cases description, results and discussion

In order to validate the INLFD code, in this section the incompressible oscillating flow is simulated for some test cases. The emphasis of this research is to investigate the capability of the developed INLFD code in predicting the details of unsteady periodic incompressible flow field and its strength in cost reduction. Although these cases are simple, they have the advantage of involving exact analytical solutions.

3.1 Case 1: Stokes second problem

In this case (Fig. 2) an infinite flat plate at the bottom of an infinitely deep sea of fluid with a linear harmonic motion parallel to itself is considered (Stokes' second problem). Since the objective is only to achieve the periodic steady solution, initial conditions are not needed to be satisfied. The velocity distribution is governed by the diffusion Eq. (13).

$$\frac{\partial u}{\partial t}=v\frac{\partial^2 u}{\partial y^2},\quad B.C.:\begin{cases}u(0,t)=U\cdot\cos(\omega t)\\ u(\infty,t)=0\end{cases} \tag{13}$$

The analytical solution of the Stokes' second problem is given by Eq. (14) [31].

$$u(y,t)=Ue^{-cy}\cos(cy-\omega t) \tag{14}$$

where $c=\sqrt{\omega/2v}$.

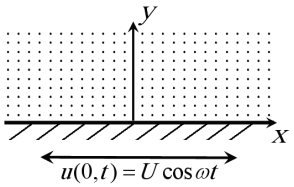

Figure 2 Coordinate system of the Stokes' second problem

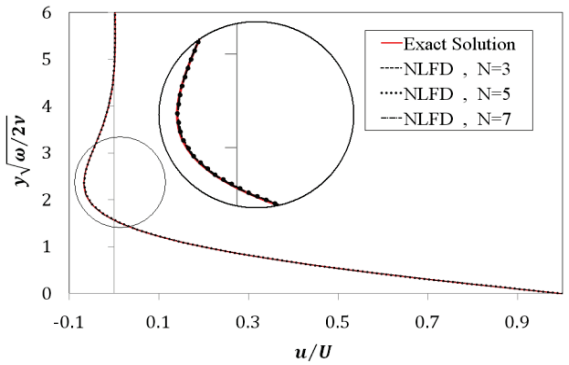

Figure 3 Velocity profile of Stokes' second problem using different harmonics

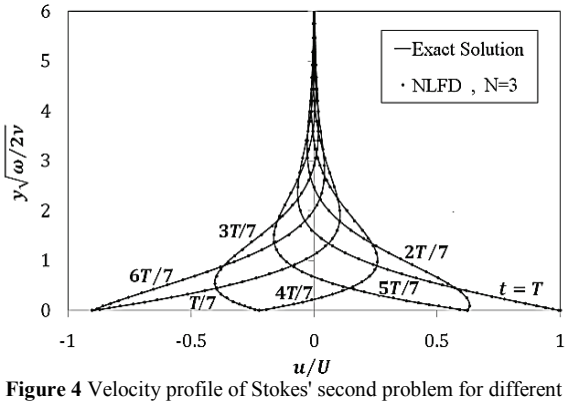

Figure 4 Velocity profile of Stokes' second problem for different instances

Moving away from the plate, the amplitude decays exponentially and the phase lag with respect to plate motion varies linearly. It means, the cosine term in Eq. (14) represents a signal propagating in y-direction while

the exponential term represents a decay in y. Fig. 3 compares the velocity profiles for 3, 5 and 7 harmonics and the exact solution at $t = T$. Since the analytical solution contains only one frequency, the numerical solution using only 3 harmonics can sufficiently provide a good estimation of the flow field. The INLFD and exact solutions are shown in Fig. 4 for different instances. As it is seen the INLFD solution completely follows the exact solution.

3.2 Case 2: Unsteady flow between two oscillating plates

In this case the motion of an incompressible viscous fluid between two infinite harmonically oscillating plates is discussed. These two plates situated at $y=\pm h$, execute harmonic oscillations in a direction parallel to themselves (Fig. 5). The flow equation is the same as Eq. (13), however the boundary conditions are different:

$$B.C.: u(\pm h, t) = U \cdot \sin(\omega t) \tag{15}$$

The analytical solution is given by Eq. (16) [32].

$$u = U \cdot \left\{ \frac{cc(yc)cc(hc) + ss(yc)ss(hc)}{cc^2(hc) + ss^2(hc)} \right\} \cdot \sin(\omega t) + \\ + U \cdot \left\{ \frac{ss(yc)cc(hc) - cc(yc)ss(hc)}{cc^2(hc) + ss^2(hc)} \right\} \cdot \cos(\omega t) \tag{16}$$

The "cc" and "ss" notations are defined as follows:

$$cc(x) = \cos(x) \cdot \cosh(x) \\ ss(x) = \sin(x) \cdot \sinh(x) \tag{17}$$

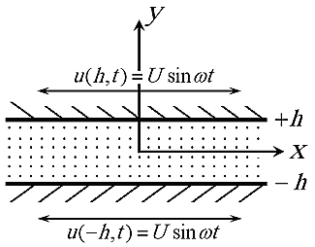

Figure 5 Geometry for unsteady flow between two oscillating plates

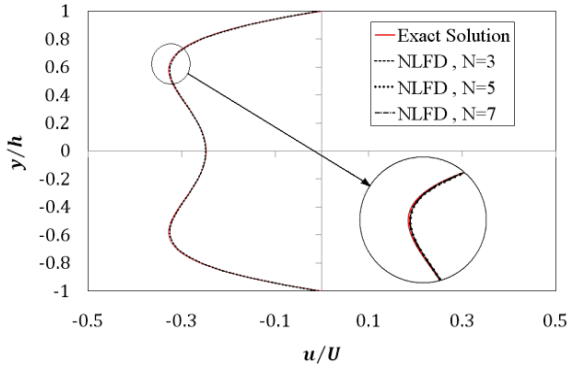

Figure 6 Velocity profile of the periodic flow between two oscillating plates using different harmonics

Fig. 6 shows the exact solution at $t = T$ and the velocity profiles for 3, 5 and 7 harmonics. According to the analytical solution, it is expected that similar to case 1, the numerical solution with 3 harmonics is adequate to provide a good approximation of the flow field. Fig. 7 shows both the exact and INLFD solutions in different instances for the flow between two oscillating plates.

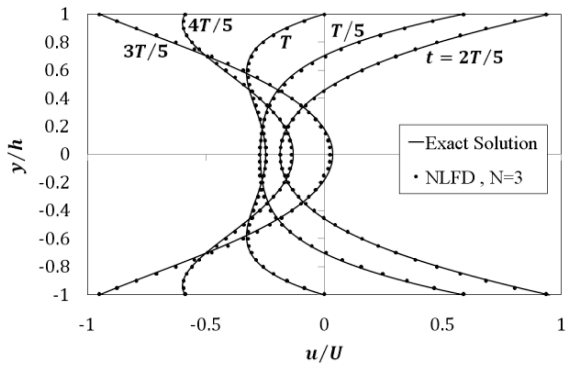

Figure 7 Velocity profile of the periodic flow between two oscillating plates for different instances

3.3 Case 3: Channel flow with a pulsatile pressure gradient

Here, two parallel static infinite plates at $y = \pm h$, with an incompressible viscous fluid between them are considered (Identical to test case 2 but with static plates).

The continuity equation is automatically satisfied and the momentum equations are reduced to:

$$\mu \frac{\partial^2 u}{\partial y^2} = \frac{\partial p}{\partial x} \tag{18}$$

where u and p are only functions of x and y, respectively. To produce a pulsating pressure gradient, an oscillating pressure can be considered:

$$p = C \cdot \cos(\omega t) \tag{19}$$

The analytical solution is then given by Eq. (20) [33].

$$u = -\frac{C}{\rho\omega} \cdot \left[\left(1 - \frac{cc(yc)cc(hc) + ss(yc)ss(hc)}{cc^2(hc) + ss^2(hc)} \right) \cdot \sin(\omega t) - \right. \\ \left. - \left(\frac{cc(yc)ss(hc) - ss(yc)cc(hc)}{cc^2(hc) + ss^2(hc)} \right) \cdot \cos(\omega t) \right] \tag{20}$$

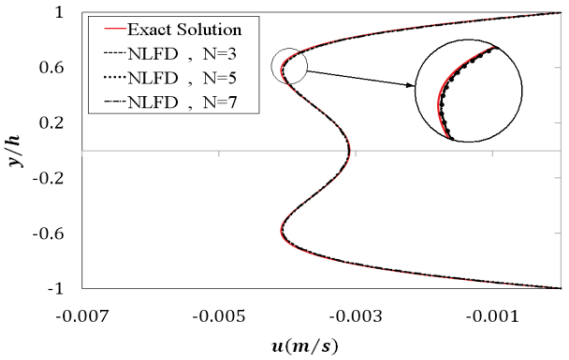

Figure 8 Velocity profile of the pulsatile pressure gradient channel flow using different harmonics

Like previous cases the numerical solution using only 3 harmonics can sufficiently provide a good

approximation of the flow field (Fig. 8). Fig. 9 illustrates the INLFD and exact solutions in different instances for the flow produced by a pulsating pressure gradient. As it is seen the INLFD solution is exactly in agreement with the analytical one.

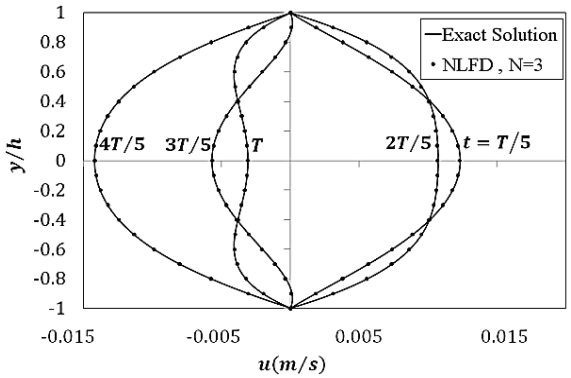

Figure 9 Velocity profile of the pulsatile pressure gradient channel flow for different instances

3.4 Case 4: Flow between two oscillating co-axial cylinders

Two infinite length concentric circular cylinders of radius r_1 and r_2 are considered (Fig. 10) and the gap between them is filled with an incompressible Newtonian fluid with kinematic viscosity, ν. The outer cup oscillates with velocity $U\cdot\cos(\omega t)$ while the inner one is kept stationary. Using polar coordinates, the continuity and momentum equations are:

$$\frac{\partial}{\partial r}\left(r\rho v_r\right)+\frac{\partial}{\partial\theta}\left(\rho v_\theta\right)=0 \tag{21a}$$

$$\frac{\partial v_r}{\partial t}+v_r\frac{\partial v_r}{\partial r}+\frac{v_\theta}{r}\frac{\partial v_r}{\partial\theta}-\frac{{v_\theta}^2}{r}=-\frac{1}{\rho}\frac{\partial p}{\partial r}+\nu\left(\nabla^2 v_r-\frac{v_r}{r^2}-\frac{2}{r^2}\frac{\partial v_\theta}{\partial\theta}\right) \tag{21b}$$

$$\frac{\partial v_\theta}{\partial t}+v_r\frac{\partial v_\theta}{\partial r}+\frac{v_\theta}{r}\frac{\partial v_\theta}{\partial\theta}+\frac{v_r v_\theta}{r}=-\frac{1}{\rho r}\frac{\partial p}{\partial\theta}+\nu\left(\nabla^2 v_\theta+\frac{2}{r^2}\frac{\partial v_r}{\partial\theta}-\frac{v_\theta}{r^2}\right) \tag{21c}$$

Since the flow is axi-symmetric, partial derivatives with respect to θ are zero and the continuity equation results in $v_r = 0$. So the momentum equations are reduced to:

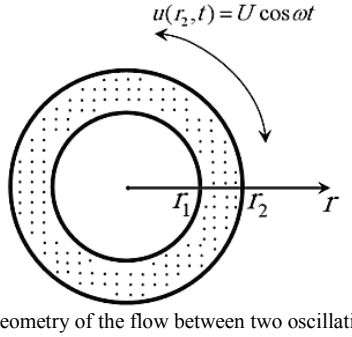

Figure 10 Geometry of the flow between two oscillating co-axial cylinders

$$\frac{\mathrm{d}p}{\mathrm{d}r}=\rho\frac{v_\theta^2}{r} \tag{22a}$$

$$\frac{\partial v_\theta}{\partial t}=\nu\left(\frac{1}{r}\frac{\partial}{\partial r}\left[r\frac{\partial v_\theta}{\partial r}\right]-\frac{v_\theta}{r^2}\right) \tag{22b}$$

Applying the separation of variables method, Eq. (22b) breaks into two independent ordinary differential equations: a t-dependent differential equation and a r-dependent one which forms a Bessel differential equation. Considering the boundary conditions, the analytical solution is:

$$v_\theta=Real\left\{e^{-i\omega t}\left[c_1J_1(\beta r)+c_2Y_1(\beta r)\right]\right\} \tag{23}$$

where $\beta=(1+i)c$ and

$$c_1=\frac{-UY_1(\beta r_1)}{Y_1(\beta r_2)J_1(\beta r_1)-J_1(\beta r_2)Y_1(\beta r_1)} \tag{24a}$$

$$c_2=\frac{UJ_1(\beta r_1)}{Y_1(\beta r_2)J_1(\beta r_1)-J_1(\beta r_2)Y_1(\beta r_1)} \tag{24b}$$

In Figs. 11 and 12 the INLFD and exact solutions are plotted in different instances for the flow between two concentric cylinders. As it is seen the INLFD solution completely follows the exact solution.

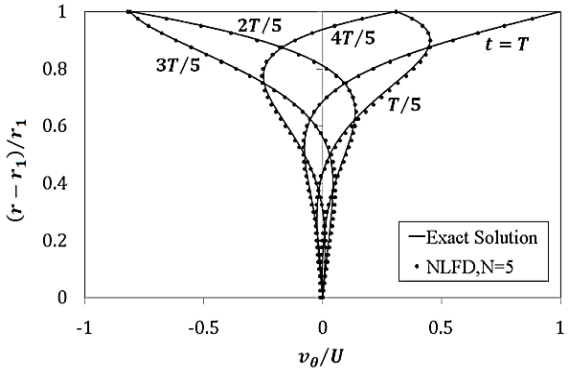

Figure 11 Velocity profile of the flow between two oscillating co-axial cylinders for different instances

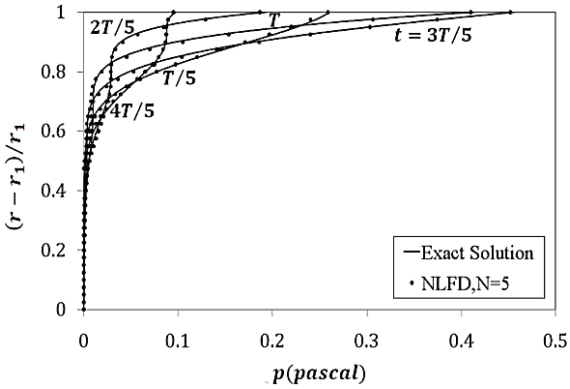

Figure 12 Pressure profile of the flow between two oscillating co-axial cylinders for different instances

Figs. 13 and 14 compare the velocity and pressure profiles for different harmonics at $t = T$ which shows using higher number of harmonics, the numerical solution

becomes closer to the exact solution. It is also seen that using 7 harmonics, the exact solution is achieved with a good approximation. Thus using higher number of harmonics is unnecessary.

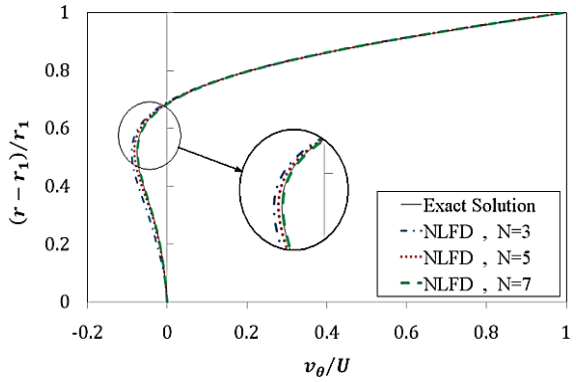

Figure 13 Velocity profile of the flow between two oscillating co-axial cylinders using different harmonics

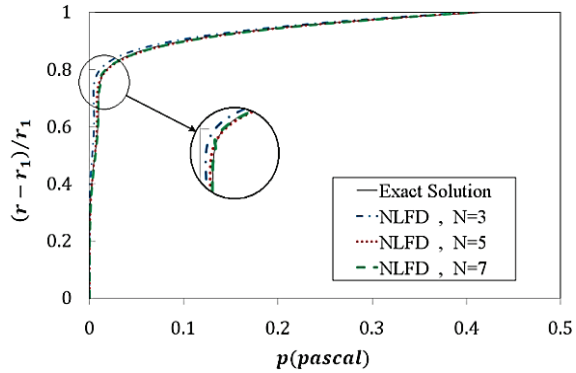

Figure 14 Pressure profile of the flow between two oscillating co-axial cylinders using different harmonics

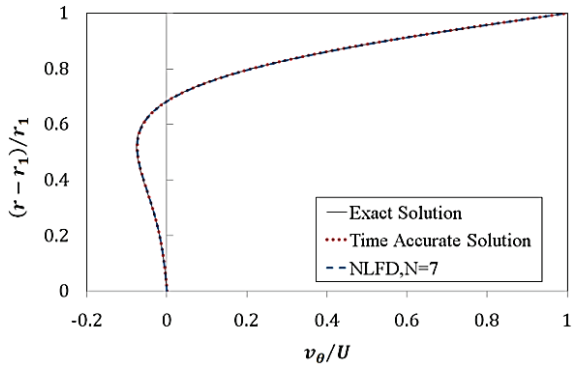

Figure 15 Velocity profile of the flow between two oscillating co-axial cylinders at $t = T$

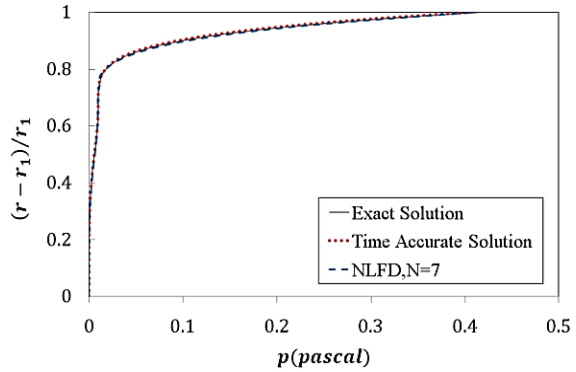

Figure 16 Pressure profile of the flow between two oscillating co-axial cylinders at $t = T$

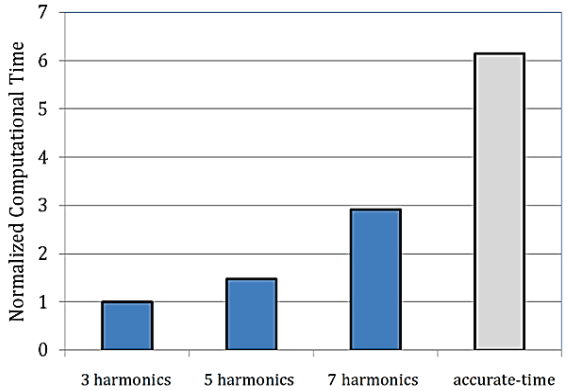

Figure 17 Normalized computational time for 3, 5 and 7 harmonics INLFD and time-accurate solutions

In order to compare the INLFD method computational cost with that of the common time-accurate methods, test case 4 is simulated with an available unsteady CFD code. In Figs. 15 and 16, the velocity and pressure profiles at $t = T$, obtained from time-accurate, INLFD ($N = 7$) and exact solutions are plotted. Fig. 17 also compares the computational time of INLFD (using different harmonics) and time-accurate solutions. Rather than demonstrating the absolute CPU time, which is machine-dependent, here the cost is presented relative to the cost of flow simulation by the INLFD code with 3 harmonics. As it is seen, 3 and 7 harmonics INLFDs are respectively six and two times faster than the time-accurate solution.

4 Conclusion

In this research a CFD code on the basis of non-linear reduced frequency domain approach was developed for simulating periodic incompressible flow. The capability of the developed INLFD code in predicting the details of the unsteady periodic incompressible flow field was then investigated. For this purpose the INLFD code validation was performed for some test cases with exact analytical solutions. For all these test cases, there was a good agreement between the INLFD code results using a limited number of time varying modes and the analytical solutions, which confirm INLFD capability to accurately resolve the flow field. The results show that capturing only the dominant harmonics can provide accurate estimations of the velocity and the pressure field. Also, it is demonstrated that the solution can be approximated with just 3 harmonics for simple cases whereas for more complex cases further harmonics (e.g. 7 harmonics in case 4) are to be used to achieve the desired level of accuracy. As an expected result, increasing the harmonics number brings about more accuracy of the INLFD solution. Afterwards the computational time reduction is also examined for one of the test cases, by comparing the INLFD cost with that of the general time dependent methods. The results show that the INLFD is approximately 2-6 times faster (based on the harmonics number used) than the time-accurate method which proves the claim of the effective computational cost reduction.

5 References

[1] Yao, J.; Davis, R.; Alonso, J. J.; Jameson, A. Unsteady Flow Investigations in an Axial Turbine Using the

Massively Parallel Flow Solver TFLO. // Technical Report 01-0529, AIAA 39th Aerospace Sciences Meeting and Exhibit / Reno, NV, January 2001.
[2] Mosahebi, A.; Nadarajah, S. An Adaptive Non-linear Frequency Domain Method for Viscous Flows. // Computers and Fluids. 75, (2013), pp. 140-154. https://doi.org/10.1016/j.compfluid.2012.12.016
[3] Mosahebi, A.; Nadarajah, S. An Implicit and Adaptive Nonlinear Frequency Domain Approach for Periodic Viscous Flows. // Journal of Computational Physics. 278, (2014), pp. 92-116. https://doi.org/10.1016/j.jcp.2014.08.022
[4] McMullen, M. The Application of Non-linear Frequency Domain Methods to the Euler and Navier–Stokes Equations. // Ph.D. thesis, Department of Aeronautics and Astronautics, Stanford University, Stanford, 2003.
[5] Verdon, J. M.; Casper, J. R.; Adamczyk, J. J. Subsonic Flow Past an Oscillating Cascade with Steady Blade Loading - Basic Formulation. // Unsteady Aerodynamics; Proceedings of the Symposium, University of Arizona, Tucson, 2(1975), pp. 827-851.
[6] Verdon, J. M.; Casper, J. R. Subsonic Flow Past an Oscillating Cascade with Finite Mean Flow Deflection. // AIAA Journal. 18, 5(1980), pp. 540-548. https://doi.org/10.2514/3.50786
[7] Whitehead, D. S. A Finite Element Solution of Unsteady Two-Dimensional Flow in Cascades. // International Journal for Numerical Methods in Fluids. 10, 1(1990), pp. 13-34. https://doi.org/10.1002/fld.1650100103
[8] Verdon, J. M.; Casper, J. R. A Linearized Unsteady Aerodynamic Analysis for Transonic Cascades. // Journal of Fluid Mechanics. 149(1984), pp. 403-429. https://doi.org/10.1017/S002211208400272X
[9] Ni, R. H.; Sisto, F. Numerical Computation of Non-stationary Aerodynamics of Flat Plate Cascades in Compressible Flow. // Transactions of the ASME, Journal of Engineering for Gas Turbine and Power. 98, 2(1976), pp. 165-170.
[10] Clark, W. S.; Hall, K. C. A Time Linearized Navier Stokes Analysis of Stall Flutter. // Transaction of ASME, Journal of Turbomachinery. 122, 3(2000), pp. 467-476. https://doi.org/10.1115/1.1303073
[11] Adamczyk, J. J. Model Equation for Simulating Flows in Multistage Turbomachinery. // ASME Paper. 85-GT-226(1984).
[12] Ning, W.; He, L. Computation of Unsteady Flows Around Oscillating Blades Using Linear and Non-Linear Harmonic Euler Methods. // Transactions of the ASME, Journal of Turbomachinery. 120, 3(1998), pp. 508-514.
[13] He, L.; Ning, W. Efficient Approach for Analysis of Unsteady Viscous Flows in Turbomachines. // AIAA Journal. 36, 11(1998), pp. 2005-2012. https://doi.org/10.2514/2.328
[14] Chen, T.; Vasanthakumar, P.; He, L. Analysis of Unsteady Blade Row Interaction using Nonlinear Harmonic Approach. // AIAA Journal of Power and Propulsion. 17, 3(2001), pp. 651-658. https://doi.org/10.2514/2.5792
[15] Thomas, J. P.; Dowell, E. H.; Hall, K. C. Nonlinear Inviscid Aerodynamic Effects on Transonic Divergence, Flutter and Limit Cycle Oscillations. // AIAA Journal. 40, 4(2002), pp. 638-646. https://doi.org/10.2514/2.1720
[16] Hall, K. C.; Thomas, J. P.; Clark, W. S. Computation of Unsteady Nonlinear Flows in Cascades Using a Harmonic Balance Technique. // AIAA Journal. 40, 5(2002), pp. 879-886. https://doi.org/10.2514/2.1754
[17] McMullen, M.; Jameson, A.; Alonso, J. Acceleration of Convergence to a Periodic Steady State in Turbomachinery Flows. // AIAA Paper 01-0152(2001).
[18] McMullen, M.; Jameson, A.; Alonso, J. Application of a Nonlinear Frequency Domain Solver to the Euler and Navier-Stokes Equations. // AIAA Paper 02-0120(2002).
[19] McMullen, M.; Jameson, A.; Alonso, J. Demonstration of Nonlinear Frequency Domain Methods. // AIAA Journal. 44, 7(2006). pp. 1428-1435. https://doi.org/10.2514/1.15127
[20] Ghasemi, S. E.; Hatami, M.; Ganji, D. D. Thermal Analysis of Convective Fin with Temperature-dependent Thermal Conductivity and Heat Generation. // Case Studies in Thermal Engineering. 4, (2014), pp. 1-8. https://doi.org/10.1016/j.csite.2014.05.002
[21] Ahmadi, A. R.; Zahmatkesh, A.; Hatami, M.; Ganji, D. D. A Comprehensive Analysis of the Flow and Heat Transfer for a Nanofluid over an Unsteady Stretching Flat Plate. // Powder Technology. 258, (2014), pp. 125-133. https://doi.org/10.1016/j.powtec.2014.03.021
[22] Hatami, M.; Domairry, G. Transient Vertically Motion of a Soluble Particle in a Newtonian Fluid Media. // Powder Technology. 253, (2014), pp. 481-485. https://doi.org/10.1016/j.powtec.2013.12.015
[23] Murman, S. M. A Reduced Frequency Approach for Calculating Dynamic Derivatives. // AIAA Journal. 45, 6(2007), pp. 1161-1168. https://doi.org/10.2514/1.15758
[24] Mavriplis, D. J.; Yang, Z.; Mundis, N.; Extensions of Time Spectral Methods for Practical Rotorcraft Problems. // AIAA Paper 12-423, 50th Aerospace Sciences Meeting and Exhibit / Nashville, TN, January 2012.
[25] Kharati Koopaee, M. Application of Non-linear Reduced Frequency Approach for Calculating Stability Derivatives in Compressible Flows. Ph.D. thesis, Department of Mechanical Engineering, Shiraz University, Shiraz, 2010.
[26] Kharati Koopaee, M.; Alishahi, M. M.; Emdad, H. An Efficient Approach for Calculation of Pitching Moment in Nonlinear Reduced Frequency Method at Low Mach Number Transonic Flows. // International Journal of Numerical Methods in Fluid. 68, 3(2012), pp.287-301. https://doi.org/10.1002/fld.2506
[27] Rempfer, D. On Boundary Conditions for Incompressible Navier-Stokes Problems. // Applied Mechanics Reviews. 59, 3(2006), pp. 107-125. https://doi.org/10.1115/1.2177683
[28] Johnston, H.; Liu, J. G. Accurate, Stable and Efficient Navier–Stokes Solvers Based on Explicit Treatment of the Pressure Term. // Journal of Computational Physics. 199, 1(2004), pp. 221-259. https://doi.org/10.1016/j.jcp.2004.02.009
[29] Peric, M.; Kessler, R.; Scheuerer, G. Comparison of Finite-Volume Numerical Methods with Staggered and Collocated Grids. // Computers & Fluids. 16, 4(1988), pp. 389-403. https://doi.org/10.1016/0045-7930(88)90024-2
[30] Patankar, S. V. Numerical Heat Transfer and Fluid Flow. Hemisphere/McGraw-Hill, 1980.
[31] Kundu, P. K.; Cohen, I. M.; Dowling, D. R. Fluid Mechanics. Academic Press, 2015.
[32] Sacheti, N. C.; Bhatt, B. S. Unsteady Flow of a Viscous Incompressible Fluid between Parallel Plates. // Defense Science Journal. 25, 2(1972), pp.147-152.
[33] Langlois, W. E.; Deville, M. O. Slow Viscous Flow. Springer, 2014. https://doi.org/10.1007/978-3-319-03835-3

Authors' addresses

Mohammad Hassan Shojaeefard, Professor
Amin Khorampanahi, Ph.D. candidate *(Corresponding author)*
Faculty of Mechanical Engineering
Iran University of Science and Technology
Narmak, Tehran, Iran, 168461
mhshf@iust.ac.ir
khorampanahi@iust.ac.ir

Masoud Kharati Koopaee, Assistant professor
Faculty of Mechanical Engineering
Shitaz University of Technology
Modares Blv., Shiraz, Iran, 715571
kharati@sutech.ac.ir